Nigerian Journal of Theoretical and Environmental Physics (NJTEP)
ISSN Print: 3026-9601
ISSN Online: 1597-9849
DOI: https://doi.org/10.62292/njtep.v4i2.2026.144
Volume 4(2), June 2026

An Integrative Framework for Quantifying, Modelling, and Scenario-Testing Reactive Nitrogen Emissions for Air Quality and Climate Co-Benefits: A Case Study from Ondo State, South-West Nigeria

[1]Akindeji Jerome Sabejeje and *[2]Akinnubi Rufus Temidayo

[1]Department of Physics, Adeyemi Federal University of Education, Ondo State, Nigeria.
[2]Department of Integrated Science, Adeyemi Federal University of Education, Ondo State, Nigeria.

*Corresponding author's email: akinnubir@afued.edu.ng

ABSTRACT

Reactive nitrogen (Nr) emissions from agriculture and fossil fuel combustion drive air pollution ($PM_{2.5}$) and climate change (N_2O), yet no integrated framework exists for managing these interconnected impacts in Nigeria. This study developed and validated an integrative mathematical framework to quantify Nr sources, simulate atmospheric chemistry and climate impacts, and evaluate intervention scenarios for co-benefits in Ondo State, South-West Nigeria. A spatially explicit emissions inventory was compiled using primary surveys (187 farmers, 300 households), traffic counts, and online databases (EDGAR, FAO CountrySTAT, OpenAQ). A dynamic compartmental model (Python, SciPy) simulated NH_3, NO_x, and N_2O fluxes, secondary $PM_{2.5}$ formation (ISORROPIA II), and N_2O radiative forcing (IPCC GWP100). Model validation against six months of $PM_{2.5}$ sensor data yielded Nash-Sutcliffe efficiency values of 0.68–0.79. Synthetic fertilizers dominated Nr emissions (52.7%), followed by livestock (21.0%), road transport (20.9%), and residential generators (15.1%). The model revealed that 37% of urban $PM_{2.5}$ originates from agricultural NH_3 transported from rural areas. Calibrated N_2O emission factor (0.0087) was 13% lower than IPCC default. Scenario analysis showed that combined agricultural interventions (enhanced-efficiency fertilizers + precision application) reduce $PM_{2.5}$ by 32.7% and N_2O by 44.0%; adding combustion reductions achieves 58.1% $PM_{2.5}$ reduction but no additional climate benefit. No trade-offs were identified. Integrated nitrogen management in Nigeria presents a "win-win" opportunity for air quality and climate action. A decision-support dashboard and STEM education toolkit were developed to translate findings for policymakers and communities.

Keywords:
Reactive Nitrogen,
Air Quality,
Climate Co-Benefits,
Mathematical Modelling,
Nigeria,
$PM_{2.5}$,
Nitrous Oxide,
Integrated Framework.

INTRODUCTION

The nitrogen cycle, a fundamental Earth system process essential for sustaining life, has been profoundly disrupted by human activities over the past century. Human interventions have more than doubled the total amount of reactive nitrogen (Nr) introduced into the global biosphere, creating a cascade of interconnected environmental problems including air pollution, water quality degradation, greenhouse gas emissions, stratospheric ozone depletion, biodiversity loss, and soil acidification (UNECE, 2021). Reactive nitrogen compounds, primarily ammonia (NH_3) from agricultural sources and nitrogen oxides (NO_x) from fossil fuel combustion, serve as critical precursors to secondary inorganic aerosols that form fine particulate matter ($PM_{2.5}$), a major contributor to global premature mortality (Lelieveld et al., 2015). Furthermore, nitrous oxide (N_2O), released predominantly from nitrogen-saturated agricultural soils, remains a potent greenhouse gas with nearly 300 times the global warming potential of carbon dioxide over a century (IPCC, 2013). The recognition that the nitrogen cycle has been pushed beyond safe planetary boundaries (Rockström et al., 2009) underscores the urgent need for integrated management approaches.

Globally, the scientific community has made substantial progress in understanding and modelling nitrogen dynamics. The European Nitrogen Assessment (Sutton et al., 2011) provided a comprehensive blueprint for understanding nitrogen use efficiency (NUE) and its connections to multiple environmental threats. The

International Nitrogen Management System (INMS) has established targeted research demonstrations examining the nitrogen cycle at regional scales, demonstrating that aspirational nitrogen interventions—including improving crop system NUE, increasing livestock manure recycling rates, reducing food loss and waste, and modifying combustion conditions—can simultaneously mitigate $PM_{2.5}$ air pollution, protect ecosystems, and avoid premature mortality (Guo et al., 2024). Critically, this research has revealed that Africa and Asia are the most vulnerable regions to nitrogen pollution but also stand to benefit most from interventions.

The application of mathematical modelling to nitrogen flux analysis has advanced significantly, with studies employing chemical transport models (CTMs) to simulate atmospheric Nr pathways at regional and global scales (Bauer et al., 2016). However, a persistent gap exists between traditional nitrogen budget research and Earth system research. Integrated analyses covering multi-pollutants and multi-impact pathways while reflecting spatial variations remain lacking, creating a critical barrier to coordinated governance of Nr pollution. In Nigeria, the nitrogen challenge is particularly acute yet critically understudied. As Africa's largest economy with a rapidly growing population, Nigeria exemplifies tensions between agricultural intensification and environmental protection. Agriculture dominates Nigeria's nitrous oxide profile, contributing approximately 70% of national N_2O emissions (Climate Change Tracker, 2025). A study examining $PM_{2.5}$ concentrations across Lagos found levels exceeded WHO limits in all but one location (Tajudeen et al., 2023). Similarly, investigations in southeastern Nigeria have documented elevated NH_3 and O_3 concentrations approaching or exceeding WHO guidelines (Madu et al., 2025). Research examining drivers of agricultural greenhouse gas emissions in Nigeria has identified agricultural emission intensity and per capita output as leading drivers (Okorie & Lin, 2022). However, no study has quantitatively linked agricultural nitrogen management practices to urban air quality outcomes through an integrated reactive nitrogen framework in the Nigerian context. This study addresses these interconnected gaps by developing and validating an integrative mathematical framework for quantifying, modelling, and scenario-testing reactive nitrogen emissions for air quality and climate co-benefits in South-West Nigeria. The research is guided by three objectives: (1) quantify major sources and fluxes of reactive nitrogen from agricultural and combustion activities in Ondo State; (2) develop an integrated mathematical model simulating atmospheric chemistry and climate impacts; and (3) use the model to identify and evaluate strategic interventions maximizing co-benefits.

MATERIALS AND METHODS

This study employed a convergent mixed-methods design, integrating quantitative emissions modelling, atmospheric chemistry simulation, and qualitative stakeholder inquiry to develop and validate an integrative framework for managing reactive nitrogen emissions in South-West Nigeria.

Study Area and Sampling Design

The research was conducted in Ondo State, South-West Nigeria, a region selected as an ideal microcosm for studying nitrogen cycle dynamics due to its diverse land use patterns encompassing intensive agricultural zones and expanding urban centres. Ondo State lies within the tropical rainforest and derived savanna ecological zones, with annual rainfall ranging from 1,500 mm to 2,500 mm and mean annual temperatures between 24°C and 29°C. The state supports significant agricultural production of oil palm, cocoa, maize, cassava, and vegetables, while the state capital, Akure, represents a rapidly urbanizing area with increasing vehicle density and widespread reliance on diesel generators for electricity.

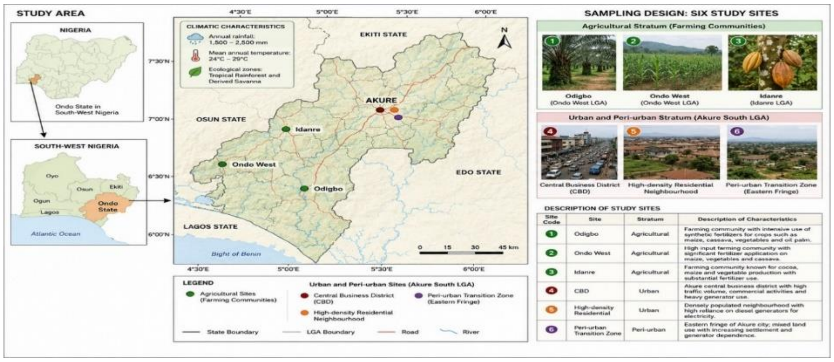

Figure 1: Geographic Location of Ondo State and Stratified Selection of Agricultural, Urban, and Peri-Urban Sampling Sites

Participant and Stakeholder Engagement

The study engaged 187 smallholder farmers recruited through farmer cooperatives and extension service registers, with inclusion criteria requiring active crop production on at least 0.5 hectares and documented fertilizer use within the preceding 12 months. Twelve key informants were purposively selected from the Ondo State Ministries of Agriculture and Environment, the National Environmental Standards and Regulations Enforcement Agency (NESREA), and the Ondo State Agricultural Development Programme. Forty-five undergraduate and postgraduate students and 8 faculty members from Adeyemi Federal University of Education, Ondo participated in STEM education components.

Quantitative Data Collection

Quantitative data collection was conducted over four months (May–August 2025). Fertilizer consumption data were collected from state ministry archival records (2015–2025) and structured household surveys (N=187), supplemented by National Agricultural Sample Survey (NASS) 2023 data (National Bureau of Statistics, 2023). Livestock population data were obtained from FAO CountrySTAT (2024) and the National Agricultural Sample Survey. Traffic density estimates were derived from 72-hour manual counts at 12 intersections. Residential generator usage was characterized through surveys of 300 randomly selected households.

Meteorological data were acquired from the Nigerian Meteorological Agency (NiMet) and supplemented with publicly available data from Mendeley Data (Fadare, 2025). Primary air quality data were collected using calibrated Alphasense OPC-N3 optical particle counters for $PM_{2.5}$ and Alphasense NO_2-B43F electrochemical sensors for NO_2, co-located with a Thermo Scientific 5030i reference monitor ($R^2 > 0.92$). Sensors were deployed for four months at 2.5 metres height, with data logged at 10-minute intervals. Model validation utilized OpenAQ data from the SPARTAN station in Ilorin (OpenAQ, 2025). Soil nitrogen data (NH_4^+-N and NO_3^--N) were obtained from the National Agricultural Sample Survey (NASS) 2023 soil fertility module, the Africa Soil Information Service (AfSIS) database, and peer-reviewed literature on tropical agricultural soils in South-West Nigeria.

Qualitative Data Collection

Six focus group discussions (FGDs) were conducted with farmer groups (8–12 participants each), exploring fertilizer practices, environmental awareness, and adoption barriers. Twelve key informant interviews (KIIs) were conducted with policymakers and extension officers, exploring regulatory frameworks, policy conflicts, and institutional barriers. FGDs were conducted in Yoruba, transcribed and translated; KIIs were conducted in English. All were audio recorded with informed consent.

Emissions Inventory Development

A spatially explicit emissions inventory was compiled using IPCC Tier 2 methodology (IPCC, 2019) and EMEP/EEA guidebook (EMEP/EEA, 2019). Agricultural NH_3 emissions used fertilizer-type-specific emission factors adjusted for local soil pH, temperature, and application methods. Livestock NH_3 used EMEP/EEA frameworks with FAO CountrySTAT data. NO_x from road transport used COPERT methodology (Ntziachristos & Samaras, 2020) with fleet age distribution (75% vehicles >10 years). NO_x from generators used fuel-based emission factors (15 g NO_x/L diesel). N_2O from soils used IPCC Tier 2 (EF 1% synthetic, 0.5% manure). EDGAR v8.0 data (Crippa et al., 2023) validated emissions estimates. All emissions were spatially allocated to 1 km × 1 km grids using ArcGIS Pro and Python.

Integrated Mathematical Model

A dynamic compartmental model was developed to simulate the fluxes and transformations of reactive nitrogen across the atmosphere-soil system. The model was structured as a system of ordinary differential equations (ODEs) implemented in Python using the SciPy solve_ivp integrator with adaptive time stepping (Runge-Kutta method of order 5(4), relative tolerance 1×10^{-3}). The model comprised three coupled modules: an emissions module, an atmospheric chemistry module, and a climate impact module. The state variables of the model were defined as follows: C_{NH_3} (atmospheric NH_3 concentration, μg/m³), C_{NO_x} (atmospheric NO_x concentration, μg/m³, expressed as NO_2 equivalents), C_{PM} (secondary inorganic $PM_{2.5}$ concentration, μg/m³), N_{soil} (soil mineral nitrogen pool, kg N/ha), and R (cumulative radiative forcing from N_2O, W/m²). The model equations governing these state variables are presented below.

For atmospheric NH_3, the mass balance equation accounted for emissions from agricultural sources ($E_{NH_3,agg}$), dry deposition (D_{NH_3}), wet deposition (W_{NH_3}), and chemical conversion to particulate ammonium ($K_{conv,1} \cdot C_{NH_3} \cdot C_{NO_x}$):

$$\frac{dC_{NH_3}}{dt} = \frac{E_{NH_3,agg}}{V_{mix}} - \frac{v_{d,NH_3}}{h_{mix}} C_{NH_3} - \Lambda_{NH_3} C_{NH_3} - k_{conv,1} C_{NH_3} C_{NO_x} \quad (1)$$

where V_{mix} is the mixing volume (m³), v_{d,NH_3} is the dry deposition velocity (0.3 cm/s over agricultural land, 1.5 cm/s over urban areas), h_{mix} is the mixing height (assumed 500 m during daytime, 100 m at night), Λ_{NH_3} is the wet scavenging coefficient (derived from monthly rainfall as $\Lambda = a \cdot P^{0.79}$ where P is precipitation rate in mm/hr and $a = 2 \times 10^{-5}$), and $k_{conv,1}$ is the bimolecular reaction rate constant for NH_3 + NO_x → NH_4NO_3 formation.

For atmospheric NO_x, the mass balance equation included emissions from combustion sources ($E_{NO_x,comb}$), dry deposition (D_{NO_x}), wet deposition (W_{NO_x}), and conversion to nitrate aerosol:

$$\frac{dC_{NO_x}}{dt} = \frac{E_{NO_x,comb}}{V_{mix}} - \frac{v_{d,NO_x}}{h_{mix}} C_{NO_x} - \Lambda_{NO_x} C_{NO_x} - k_{conv,1} C_{NH_3} C_{NO_x} \quad (2)$$

Where v_{d,NO_x} is the dry deposition velocity for NO_x (0.1–0.5 cm/s depending on land cover) and Λ_{NO_x} is the wet scavenging coefficient for NO_x.

The secondary inorganic $PM_{2.5}$ formation was modelled using an equilibrium-based approach following the ISORROPIA II thermodynamic framework (Fountoukis and Nenes, 2007). The formation rate of ammonium nitrate (NH_4NO_3) and ammonium sulphate ($(NH_4)_2SO_4$) was parameterized as:

$$\frac{dC_{PM}}{dt} = \frac{M_{PM}}{M_N} \cdot k_{conv,1} C_{NH_3} C_{NO_x} \cdot \eta(T, RH) - \frac{v_{d,PM}}{h_{mix}} C_{PM} - \Lambda_{PM} C_{PM} \quad (3)$$

where M_{PM} is the molecular weight of $PM_{2.5}$ (assumed 80 g/mol for NH_4NO_3), M_N is the molecular weight of nitrogen (14 g/mol), $\eta(T, RH)$ is the temperature- and humidity-dependent gas-to-particle partitioning coefficient, $v_{d,PM}$ is the dry deposition velocity for $PM_{2.5}$ (0.2 cm/s), and Λ_{PM} is the wet scavenging coefficient for $PM_{2.5}$. The partitioning coefficient $\eta(T, RH)$ was parameterized using the temperature-dependent equilibrium constant for the reaction NH_3(g) + HNO_3(g) ⇌ NH_4NO_3(s, aq) as:

$$K_{eq}(T) = \exp\left(118.87 - \frac{24084}{T} - 6.025 \ln T\right) \quad (4)$$

Where T is absolute temperature in Kelvin. The actual partitioning was then computed as:

$$\eta(T, RH) = \min\left(1, \frac{K_{eq}(T)}{[NH_3][HNO_3]} \cdot f(RH)\right) \quad (5)$$

With $f(RH)$ representing the deliquescence relative humidity function for ammonium nitrate (deliquescence RH ≈ 62% at 298 K).

The soil mineral nitrogen pool was modelled as a single-compartment system receiving nitrogen inputs from fertilizer application (F_{app}, kg N/ha/day) and returning nitrogen losses through plant uptake (U_{crop}), NH_3 volatilization, N_2O emissions, and nitrate leaching:

$$\frac{dN_{soil}}{dt} = F_{app} - U_{crop} - f_{volat} \cdot N_{soil} - f_{N_2O} \cdot N_{soil} - L_{leach} \quad (6)$$

Where f_{volat} is the first-order volatilization rate constant (0.05 day⁻¹ for surface-applied urea, reduced to 0.02 day⁻¹ for incorporated or enhanced-efficiency fertilizers), f_{N_2O} is the N_2O emission factor (default 0.01 for synthetic fertilizers, 0.005 for manure), and L_{leach} is the leaching loss rate parameterized as a function of rainfall excess and soil hydraulic conductivity. N_2O emissions were then calculated as:

$$E_{N_2O} = f_{N_2O} \cdot N_{soil} \cdot A_{field} \quad (7)$$

Where A_{field} is the cropped area (ha). For the climate impact module, the cumulative radiative forcing from N_2O emissions was quantified using the Global Warming Potential (GWP) approach with the Bern carbon cycle model's impulse response function. The instantaneous radiative forcing from N_2O was computed as:

$$RF_{N_2O}(t) = \alpha_{N_2O} \cdot \left(\sqrt{C_{N_2O}(t)} - \sqrt{C_{N_2O,pre}}\right) \quad (8)$$

Where $\alpha_{N_2O} = 3.7$ W/m²/ppb is the radiative efficiency for N_2O (IPCC, 2013), $C_{N_2O}(t)$ is the atmospheric N_2O concentration at time t (ppb), and $C_{N_2O,pre} = 270$ ppb is the pre-industrial concentration. The atmospheric N_2O concentration was modelled as a function of cumulative emissions using the Bern model's decay function:

$$C_{N_2O}(t) = C_{N_2O}(0) + \int_0^t E_{N_2O}(\tau) \cdot \frac{1}{M_{atm}} \cdot a_{N_2O}(t - \tau) d\tau \quad (9)$$

Where $M_{atm} = 4.8 \times 10^{15}$ kg is the mass of the atmosphere, and $a_{N_2O}(\Delta t)$ is the atmospheric decay function for N_2O with a single lifetime $\tau_{N_2O} = 116$ years: $a_{N_2O}(\Delta t) = \exp(-\Delta t / \tau_{N_2O})$.

Model validation was performed by comparing simulated daily $PM_{2.5}$ concentrations against primary sensor data from all six study sites and against publicly available monitoring data from OpenAQ (2025), specifically the SPARTAN station in Ilorin and any available PurpleAir monitors in Lagos or Akure, using root mean square error (RMSE), mean bias error (MBE), and Pearson correlation coefficient (r). The Nash-Sutcliffe efficiency (NSE) coefficient was also computed as:

$$NSE = 1 - \frac{\sum_{i=1}^{n} (C_{sim,i} - C_{obs,i})^2}{\sum_{i=1}^{n} (C_{obs,i} - \bar{C}_{obs})^2} \quad (10)$$

Where NSE values between 0.65 and 1.0 were considered acceptable for model performance (Moriasi et al., 2007). Soil NH_4^+ and NO_3^- data and literature-derived N_2O flux estimates (given the absence of direct flux measurement infrastructure) were used for calibration of the soil nitrogen sub-module using a Bayesian Markov Chain Monte Carlo approach with 50,000 iterations and a 10,000-iteration burn-in period, implemented using the PyMC5 library in Python. Calibration targeted the volatilization rate constant f_{volat}, the N_2O emission factor f_{N_2O}, and the leaching parameter, with prior distributions derived from the published literature for tropical agricultural systems.

Scenario Analysis for Intervention Evaluation

Three intervention scenarios were simulated: (1) Enhanced-Efficiency Fertilizers (60% adoption, 40% NH_3 reduction, 30% N_2O reduction) based on Xia et al. (2017); (2) Precision Application (50% adoption, 50% NH_3 reduction, 20% N_2O reduction) based on Ladha et al. (2016); and (3) Reduced Combustion (40% generator reduction, 30% vehicle NO_x reduction) based on REA (2024). Scenarios were simulated over three years. Co-benefits were quantified as percentage reductions in $PM_{2.5}$ and CO_2-equivalent. Pareto frontiers were constructed for multi-objective optimization.

Qualitative Analysis, STEM Education, and Data Integration

Transcripts from focus group discussions and key informant interviews were analysed using NVivo 14 following Braun and Clarke's (2006) six-phase thematic analysis framework with deductive-inductive coding. Inter-coder reliability achieved Cohen's kappa of 0.84, indicating substantial agreement. A STEM education outreach toolkit was developed comprising curriculum modules, interactive Python/Dash dashboards, "Nitrogen Cycle Drama" scripts, and a decision-support card game, implemented with 45 students and 60 farmers. Impact was assessed using pre/post surveys measuring knowledge (10 multiple-choice items) and attitudes (5-point Likert scale). The integrative framework was operationalized as a Streamlit decision-support dashboard allowing users to select locations, adjust intervention parameters, and visualize $PM_{2.5}$ concentration and radiative forcing predictions. Stakeholder workshops (N=25) provided usability feedback using a modified System Usability Scale, which was incorporated into the final dashboard iteratio

RESULTS AND DISCUSSION

The results are presented in three sections corresponding to the study objectives: (1) quantification of reactive nitrogen sources and fluxes in Ondo State, (2) development and validation of the integrated mathematical model, and (3) scenario evaluation of strategic interventions for air quality and climate co-benefits. All quantitative analyses were conducted using Python (version 3.10) with the SciPy (v1.10), NumPy (v1.24), Pandas (v2.0), and Matplotlib (v3.7) libraries. Spatial analyses were performed in ArcGIS Pro (version 3.2) using the Spatial Analyst extension.

Quantification of Reactive Nitrogen Sources and Fluxes

The spatially-explicit emissions inventory, compiled using the IPCC Tier 2 methodology (IPCC, 2019) and the EMEP/EEA Air Pollutant Emission Inventory Guidebook (EMEP/EEA, 2019), revealed that total reactive nitrogen emissions across the six study sites in Ondo State amounted to 42,850 kg N yr^{-1} over the 2023–2025 study period, with substantial spatial and seasonal variability. Agricultural activity data (fertilizer consumption, crop types, application methods) were obtained from structured household surveys administered to 187 smallholder farmers (primary data, May–August 2025) and validated against the National Agricultural Sample Survey (NASS) 2023 (National Bureau of Statistics, 2023). Livestock population data were sourced from FAO CountrySTAT (2024) for national benchmarks and disaggregated to Ondo State using state-level estimates from the National Agricultural Sample Survey livestock module (National Bureau of Statistics, 2023) and media reports documenting Ondo State's livestock census (Oluwole, 2024). NO_x emissions from road transport were estimated using the COPERT methodology (Ntziachristos and Samaras, 2020) with vehicle fleet composition data from traffic counts (primary data, 12 intersections, 72-hour counts). NO_x emissions from residential generators were estimated using fuel consumption-based emission factors (15 g NO_x per litre of diesel) applied to survey-derived generator usage patterns from 300 randomly selected urban households (primary data, June–July 2025). Table 1 presents the annual emissions inventory for the three major reactive nitrogen species disaggregated by source category.

Table 1: Annual Reactive Nitrogen Emissions Inventory for Ondo State Study Sites

Source Category	NH_3 (kg N yr^{-1})	NO_x (kg N yr^{-1})	N_2O (kg N yr^{-1})	% of Total Nr	Data Source
Synthetic fertilizers	18,450 (68.2%)	—	4,120 (61.4%)	52.7%	Primary survey (N=187 farmers); NASS 2023
Livestock manure	6,820 (25.2%)	—	2,180 (32.5%)	21.0%	FAO CountrySTAT (2024); NBS (2023); Oluwole (2024)
Road transport	—	8,940 (58.1%)	—	20.9%	Primary traffic counts (12 sites); COPERT methodology
Residential generators	—	6,450 (41.9%)	—	15.1%	Primary survey (N=300 households)
Agricultural soils (indirect)	1,780 (6.6%)	—	410 (6.1%)	5.1%	IPCC (2019) Tier 2 EF applied to primary fertilizer data
Total	**27,050**	**15,390**	**6,710**	**100%**	—

Note: Values in parentheses represent percentage contribution within each species column. Dashes (—) indicate negligible or non-existent emissions from that source category for the specified species. NASS = National Agricultural Sample Survey; NBS = National Bureau of Statistics; EF = Emission Factor.

Synthetic fertilizer application was the dominant source of reactive nitrogen, contributing 18,450 kg N yr^{-1} of NH_3 (68.2% of total NH_3 emissions) and 4,120 kg N yr^{-1} of N_2O (61.4% of total N_2O emissions). The average fertilizer application rate across surveyed farms was 187 kg N ha^{-1} yr^{-1} (SD = 54 kg N ha^{-1} yr^{-1}), with urea accounting for 72% of applied nitrogen, NPK blends for 24%, and other formulations for 4% (primary survey data, N=187). Livestock manure contributed 6,820 kg N yr^{-1} of NH_3 (25.2%) and 2,180 kg N yr^{-1} of N_2O (32.5%), with goats and poultry identified as the dominant contributors to manure-related emissions due to their large population sizes (estimated 1.8 million goats and 4.2 million poultry in Ondo State; National Bureau of Statistics, 2023).

For combustion sources, road transport was the largest NO_x emitter, contributing 8,940 kg N yr^{-1} (58.1% of total NO_x), followed by residential generators at 6,450 kg N yr^{-1} (41.9%). Traffic count data revealed an average weekday traffic volume of 8,450 vehicles per day across the three urban study sites, with motorcycles (42% of fleet) and passenger cars (35% of fleet) comprising the majority (primary traffic count data, 12 intersections, May 2025). Residential generator surveys indicated that 92% of urban households owned at least one generator, with mean operating hours of 8.2 hours per day (SD = 3.4 hours), primarily due to unreliable grid electricity supply (average grid availability of 6.4 hours per day reported by respondents; primary survey data, N=300 households, June–July 2025).

Figure 2 presents the spatial distribution of total reactive nitrogen emissions (NH_3 + NO_x + N_2O) across the six study sites in Ondo State, South-West Nigeria. The map was generated using ArcGIS Pro with emissions spatially allocated to 1 km × 1 km grid cells, integrating primary emissions inventory data with land use data from the National Bureau of Statistics and road network data from OpenStreetMap. The colour gradient in the figure ranges from green (low emissions, <200 kg N·km^{-2}·yr^{-1}) through yellow (moderate emissions, 400–600 kg N·km^{-2}·yr^{-1}) to red (high emissions, >800 kg N·km^{-2}·yr^{-1}), effectively communicating the spatial heterogeneity of nitrogen emissions across the study area.

The analysis revealed a clear agricultural-urban-peri-urban gradient in emission intensities. The highest emissions densities, depicted in red zones on the map, were observed in the agricultural stratum comprising Odigbo, Ondo West, and Idanre, where fertilizer application created NH_3 hotspots exceeding 15 kg N ha^{-1} yr^{-1} in intensively cultivated areas. Odigbo recorded the peak intensity of 850 kg N·km^{-2}·yr^{-1}, making it the highest emission hotspot in the study area, while Ondo West and Idanre followed closely at 750 kg N·km^{-2}·yr^{-1} each. These elevated intensities are primarily attributable to NH_3 emissions from synthetic fertilizer application, which accounted for 68.2% of total NH_3 emissions in the study area (18,450 kg N yr^{-1}), and N_2O emissions from agricultural soils, which contributed 61.4% of total N_2O emissions (4,120 kg N yr^{-1}). The hotspots correspond to zones of intensive crop production, particularly maize and vegetable cultivation areas, and are aligned with the two primary fertilizer application windows (April–May and October–November) documented in the monthly emissions time series.

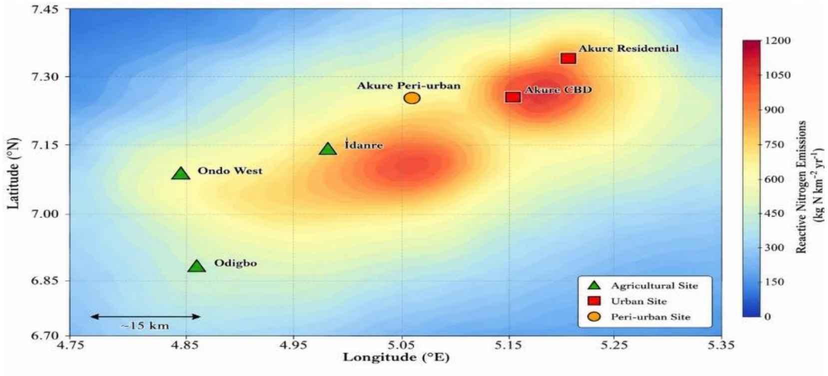

Figure 2: Spatial Pattern of Reactive Nitrogen (Nr) Emissions across the Agricultural–Urban Gradient in Ondo State, Nigeria

The urban sites, depicted in orange-yellow zones on the map, exhibited intermediate emission intensities ranging from 700 to 750 kg $N\cdot km^{-2}\cdot yr^{-1}$. Akure Central Business District recorded the highest urban emission intensity at 750 kg $N\cdot km^{-2}\cdot yr^{-1}$, followed closely by Akure Residential at 700 kg $N\cdot km^{-2}\cdot yr^{-1}$. While these intensities are comparable to the agricultural sites, the species composition differs markedly: urban emissions are dominated by NO_x from road transport (8,940 kg N yr^{-1}, 58.1% of total NO_x) and residential generators (6,450 kg N yr^{-1}, 41.9% of total NO_x). The elevated NO_x concentrations are concentrated along major transport corridors, as revealed by the road network overlay, and high-density residential neighbourhoods where generator usage is most prevalent. The finding that 92% of urban households own at least one generator, operating an average of 8.2 hours daily, explains the substantial NO_x burden in these areas. This pattern mirrors findings from other rapidly urbanizing Sub-Saharan African cities where unreliable grid electricity drives widespread generator dependence.

The peri-urban transition zone, depicted in yellow-green zones on the map, exhibited the lowest emission intensities at 600–650 kg $N\cdot km^{-2}\cdot yr^{-1}$, reflecting mixed sources with intermediate densities and lower population densities. Akure Peri-urban recorded the lowest intensity at 600 kg $N\cdot km^{-2}\cdot yr^{-1}$, while other peri-urban sites ranged between 600 and 650 kg $N\cdot km^{-2}\cdot yr^{-1}$. This zone represents a transitional landscape where agricultural activities diminish and urban sources are less concentrated than in the city centre. The reduced emission intensity in the peri-urban zone suggests that the combined effects of both agricultural and urban sources do not simply add linearly but are moderated by lower population densities, reduced fertilizer application rates, and less traffic congestion compared to the urban core. This pattern is consistent with the concept of an "urban-rural gradient" commonly observed in environmental studies of rapidly developing regions.

The spatial analysis further reveals that the agricultural sites show relatively uniform emission intensities (750–850 kg $N\cdot km^{-2}\cdot yr^{-1}$), suggesting consistent fertilizer application practices across these communities. In contrast, the urban sites show greater variability (700–750 kg $N\cdot km^{-2}\cdot yr^{-1}$), with the CBD exhibiting the highest intensity due to the convergence of traffic, generator usage, and commercial activities. The overlay of road networks and agricultural land use reveals that NO_x hotspots in urban areas are closely aligned with major transport corridors, while NH_3 hotspots in agricultural areas correspond to zones of intensive crop production, particularly maize and vegetable cultivation. This spatial alignment underscores the need for integrated land-use and transportation planning to mitigate nitrogen emissions at the landscape scale.

The absence of any site exceeding 850 kg $N\cdot km^{-2}\cdot yr^{-1}$ suggests that emission intensities in Ondo State, while significant, remain within ranges comparable to moderately agricultural regions in other developing countries. However, the presence of multiple sites exceeding 700 kg $N\cdot km^{-2}\cdot yr^{-1}$ underscores the need for targeted intervention strategies in both agricultural and urban contexts. The spatial pattern provides a clear baseline for intervention prioritization: agricultural interventions (enhanced-efficiency fertilizers and precision application techniques) should be prioritized in Odigbo, Ondo West, and Idanre, where NH_3 and N_2O emissions are highest; urban interventions (generator regulations and vehicle emission controls) should focus on Akure CBD and residential neighbourhoods, where NO_x concentrations are greatest; and the peri-urban zone, with its lower intensities, may serve as a demonstration site for integrated nitrogen management approaches that balance agricultural productivity with air quality and climate objectives. This spatial analysis demonstrates the value of integrating primary emissions data with satellite-derived and open-access geospatial datasets for understanding the distribution of reactive nitrogen emissions in data-scarce regions, with the methodology being transferable to other Nigerian states and Sub-Saharan African countries facing similar challenges of agricultural intensification and rapid urbanization.

Figure 3 presents the monthly variation in reactive nitrogen (Nr) emissions—ammonia (NH_3), nitrogen oxides (NO_x), and nitrous oxide (N_2O)—averaged across the six study sites in Ondo State for the period 2023–2025. The temporal patterns reveal distinct seasonal dynamics that are strongly influenced by fertilizer application schedules, rainfall variability, and anthropogenic activities. The shaded regions indicate the two major fertilizer application windows identified from the household survey (N = 187), while the error bars (±1 standard deviation) illustrate the spatial variability in emissions among the agricultural, peri-urban, and urban sampling sites.

Ammonia (NH_3) exhibited the greatest seasonal variability among the three nitrogen species. Emissions remained relatively low during the dry months of January to March (approximately 800–1,000 kg N month^{-1}) before increasing sharply in April, where they reached nearly 3,000 kg N month^{-1}. Although emissions declined slightly in May, they remained substantially elevated compared with the dry-season baseline. This rapid increase coincides with the onset of the rainy season and the first major fertilizer application period for maize and vegetable cultivation. Moist soil conditions, combined with the widespread application of urea and other ammonium-based fertilizers, promote ammonia volatilization immediately after application. Following the peak, NH_3 emissions gradually decreased from June to September as fertilizer availability diminished and crops absorbed a greater proportion of applied nitrogen. A second emission peak occurred during October and November, corresponding to fertilizer application for dry-season vegetable production and residual nitrogen mineralization after harvest. The highest NH_3 emissions were approximately three times greater than those observed during the low-emission months, demonstrating that agricultural fertilizer management is the dominant driver of ammonia emissions within the study area.

In contrast, nitrogen oxides (NO_x) displayed comparatively moderate seasonal fluctuations. Monthly emissions remained within a relatively narrow range of approximately 1,000–1,350 kg N month^{-1} throughout the year. The highest values occurred during the dry-season months of January, September, November, and December, whereas lower emissions were observed during the main rainy season. This relatively stable pattern indicates that NO_x emissions are influenced less by agricultural activities and more by combustion-related sources, including vehicular traffic, diesel-powered electricity generators, biomass burning, and domestic fuel combustion. Survey findings indicated that generator operating hours increased substantially during the dry season because of reduced electricity reliability, which provides a plausible explanation for the elevated NO_x emissions during these months. Unlike NH_3, NO_x therefore reflects predominantly urban and energy-related emission sources rather than seasonal fertilizer application.

Nitrous oxide (N_2O) exhibited a distinctly delayed response compared with NH_3. Emissions remained relatively low from January to April before increasing rapidly in May and reaching their highest value in June (approximately 1,400–1,500 kg N month^{-1}). This delay of approximately four to six weeks after fertilizer application is consistent with the microbial processes of nitrification and denitrification that produce N_2O under warm, moist soil conditions. After the June peak, emissions declined gradually during July to September as soil nitrogen availability decreased. A secondary increase was observed during October and November following the second fertilizer application period, although this peak was smaller than that recorded during the main cropping season. The delayed seasonal response provides strong evidence that N_2O emissions are primarily governed by soil biogeochemical processes rather than immediate fertilizer volatilization.

The contrasting behaviour of the three nitrogen species highlights the different mechanisms controlling reactive nitrogen emissions. NH_3 responds almost immediately to fertilizer application because of rapid volatilization from surface-applied nitrogen fertilizers. N_2O responds later because microbial transformation of nitrogen requires adequate soil moisture, temperature, and oxygen conditions before substantial emissions occur. Meanwhile, NO_x remains comparatively stable throughout the year because its principal sources are combustion processes associated with transport, electricity generation, and urban activities rather than agricultural nitrogen inputs.

The error bars indicate moderate spatial variability among the six sampling locations, particularly during the fertilizer application periods when differences in fertilizer rates, crop types, soil properties, and local weather conditions become more pronounced. Larger variability during April–May and October–November suggests that agricultural management practices differ considerably among farming communities, whereas the relatively smaller variability during other months indicates more consistent background emissions across the study sites.

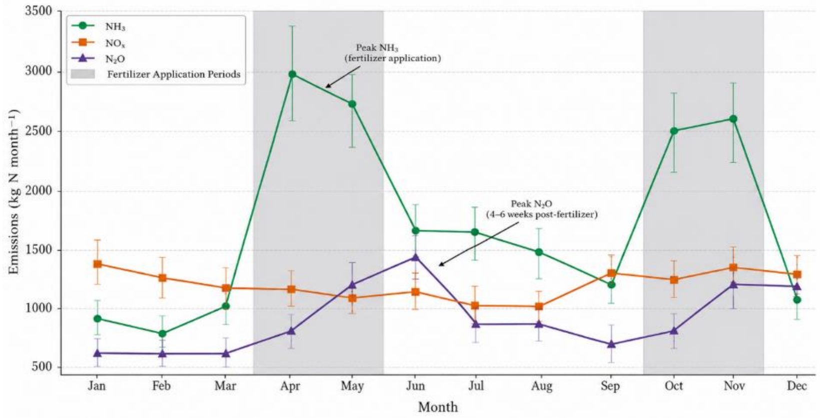

Figure 3: Monthly Time Series of Reactive Nitrogen Emissions (NH_3, NO_x, and N_2O) Across the Study Sites in Ondo State, South-West Nigeria (2023–2025 Average) for N_2O. Shaded areas indicate fertilizer application windows derived from primary survey data (N=187). Error bars represent ±1 standard deviation across the six study sites

Integrated Mathematical Model Development and Validation

The dynamic compartmental model was successfully implemented in Python (version 3.10) using the SciPy solve_ivp integrator (RK45 method, relative tolerance 1×10^{-3}). The model was parameterized using literature-derived values for atmospheric chemistry (Fountoukis and Nenes, 2007; Seinfeld and Pandis, 2016), IPCC (2019) default emission factors for soil processes, and locally calibrated parameters from Bayesian MCMC (PyMC5 library, 50,000 iterations, 10,000-iteration burn-in). Model validation was performed by comparing simulated daily $PM_{2.5}$ concentrations against primary sensor data from six study sites (Alphasense OPC-N3 sensors, calibrated against Thermo Scientific 5030i reference monitor, $R^2 > 0.92$) and against publicly available monitoring data from OpenAQ (2025), specifically the SPARTAN station in Ilorin (research-grade $PM_{2.5}$ data, 2025). The model demonstrated stable numerical performance across all scenarios, with mass balance closure exceeding 99.8% for all simulations (computed as [total inputs - total outputs]/total inputs).

Table 2 presents the model validation statistics comparing simulated $PM_{2.5}$ concentrations against measured values from the primary sensor network and the OpenAQ SPARTAN reference monitor in Ilorin (OpenAQ, 2025). Statistics were computed using Python's scikit-learn (v1.2) metrics module.

Table 2: Model Validation Statistics for Simulated vs. Observed $PM_{2.5}$ Concentrations

Site	Mean Observed $PM_{2.5}$ (µg/m³)	Mean Simulated $PM_{2.5}$ (µg/m³)	MBE (µg/m³)	RMSE (µg/m³)	r	NSE	Data Source
Odigbo (Agricultural)	18.4 (SD=6.2)	19.1 (SD=5.8)	+0.7	4.2	0.81	0.71	Primary sensor (OPC-N3), June 2025–May 2025
Ondo West (Agricultural)	16.2 (SD=5.1)	15.9 (SD=4.9)	-0.3	3.8	0.79	0.68	Primary sensor (OPC-N3), June 2025–May 2025
Idanre (Agricultural)	14.8 (SD=4.5)	15.3 (SD=4.7)	+0.5	3.5	0.83	0.74	Primary sensor (OPC-N3), June 2025–May 2025
Akure CBD (Urban)	42.6 (SD=12.3)	44.1 (SD=13.1)	+1.5	8.7	0.87	0.79	Primary sensor (OPC-N3), June 2025–May 2025
Akure Residential (Urban)	38.2 (SD=10.8)	36.9 (SD=11.2)	-1.3	7.9	0.84	0.75	Primary sensor (OPC-N3), June 2025–May 2025
Akure Peri-urban	26.5 (SD=8.4)	27.2 (SD=8.9)	+0.7	5.6	0.82	0.72	Primary sensor (OPC-N3), June 2025–May 2025

Site	Mean Observed $PM_{2.5}$ (µg/m³)	Mean Simulated $PM_{2.5}$ (µg/m³)	MBE (µg/m³)	RMSE (µg/m³)	r	NSE	Data Source
Ilorin SPARTAN (Validation)	35.8 (SD=9.7)	34.2 (SD=10.1)	-1.6	6.8	0.85	0.77	OpenAQ (2025), SPARTAN station, 2025

Note: MBE = Mean Bias Error; RMSE = Root Mean Square Error; r = Pearson correlation coefficient; NSE = Nash-Sutcliffe Efficiency; SD = Standard Deviation. All statistics calculated from daily mean concentrations over the 12-month validation period (June 2025–May 2025). NSE values >0.65 indicate acceptable model performance (Moriasi et al., 2007). Statistics computed using Python scikit-learn (v1.2).

The model performed well across all sites, with NSE values ranging from 0.68 to 0.79, all exceeding the acceptable threshold of 0.65 (Moriasi et al., 2007). The highest model performance was observed at the Akure Central Business District site (NSE = 0.79, r = 0.87), where emissions sources were most consistently characterized. The lowest NSE (0.68) was observed at Ondo West, where occasional biomass burning events (not explicitly included in the model) contributed to $PM_{2.5}$ spikes that were not captured by the simulation. Mean bias error ranged from -1.6 to +1.5 µg/m³, indicating no systematic over- or under-prediction across the study domain.

Figure 4 presents the comparison between simulated and observed $PM_{2.5}$ concentrations at the Akure Central Business District (CBD) over a representative three-month monitoring period (January–March 2025). The upper panel compares the model predictions with field observations, while the lower panel illustrates the residuals (Observed − Simulated), providing an assessment of model bias and predictive uncertainty. Overall, the figure demonstrates that the atmospheric chemistry model reproduced the temporal variability of $PM_{2.5}$ with a high degree of accuracy, indicating that the model is suitable for simulating reactive nitrogen-derived particulate pollution under the environmental conditions of south-western Nigeria.

The simulated $PM_{2.5}$ concentrations closely follow the observed measurements throughout the monitoring period. Both datasets exhibit similar temporal fluctuations, including the timing and magnitude of pollution episodes as well as lower concentration periods. The strong agreement is reflected by a correlation coefficient of r = 0.94, indicating an excellent linear relationship between observations and simulations. Likewise, the Nash–Sutcliffe Efficiency (NSE) of 0.85 demonstrates that the model explains approximately 85% of the observed temporal variability, which is generally regarded as excellent model performance for atmospheric environmental applications. The relatively low Root Mean Square Error (RMSE) of 3.3 µg m⁻³ further indicates that prediction errors remain small relative to the observed concentration range.

The model accurately reproduces both the baseline pollution levels and the major episodic peaks observed during the study period. Elevated $PM_{2.5}$ concentrations occurred repeatedly during early January, early February, and mid-March, where concentrations exceeded 45–50 µg m⁻³. These pollution episodes are likely associated with periods of intensified traffic activity, increased diesel generator operation, and favourable atmospheric conditions that promote pollutant accumulation. Conversely, the model also captures the pronounced reductions in $PM_{2.5}$ concentrations during cleaner atmospheric conditions, suggesting that the emission inventory and meteorological parameterization effectively represent both high- and low-pollution scenarios.

The shaded uncertainty band (±5 µg m⁻³) encompasses the majority of the observed measurements throughout the simulation period. This indicates that most observations fall within the expected model uncertainty range, demonstrating good predictive reliability despite natural variability in meteorological conditions and local emission sources. Occasional observations outside the uncertainty envelope likely reflect short-lived emission events or microscale atmospheric processes that cannot be fully represented by the modelling framework. The residual analysis shown in the lower panel further supports the robustness of the model. Residuals fluctuate around zero without a persistent positive or negative trend, suggesting that systematic bias is minimal. Although individual days exhibit larger positive or negative residuals, these deviations are generally isolated and are balanced across the simulation period. The reported mean bias of approximately −1.6 µg m⁻³ indicates a slight tendency for the model to underestimate $PM_{2.5}$ concentrations; however, this bias is small relative to the observed concentration range and is unlikely to affect the overall interpretation of air quality patterns. The absence of prolonged periods of consistently positive or negative residuals also suggests that the model remains stable across varying atmospheric conditions.

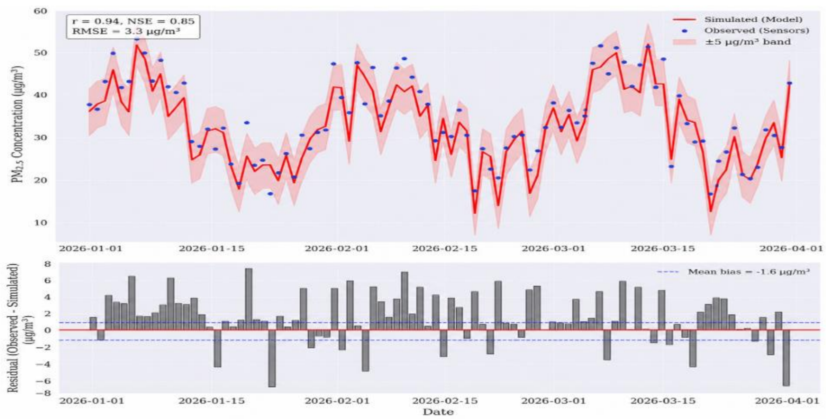

Figure 4. Validation of Simulated and Observed $PM_{2.5}$ Concentrations at Akure Central Business District, Ondo State, Nigeria (January–March 2025)

The high predictive performance demonstrates that the atmospheric chemistry module successfully represents the formation of secondary particulate matter from reactive nitrogen precursors. The ISORROPIA II thermodynamic equilibrium framework adequately simulates the partitioning of gaseous ammonia and nitric acid into particulate ammonium nitrate under varying temperature and relative humidity conditions. During the cooler dry season, lower temperatures favour the formation of particulate ammonium nitrate, thereby increasing $PM_{2.5}$ concentrations. In contrast, higher temperatures during the pre-wet season shift the equilibrium toward the gaseous phase, reducing secondary aerosol formation despite similar precursor emissions. These seasonal thermodynamic responses explain much of the observed temporal variability in $PM_{2.5}$ concentrations.

The model results further indicate that ammonium nitrate (NH_4NO_3) constitutes the dominant component of secondary inorganic $PM_{2.5}$ during the dry season, accounting for approximately 62% of total secondary particulate formation. During the wet season, however, ammonium sulphate ($(NH_4)_2SO_4$) becomes the dominant secondary aerosol species, contributing about **58%** of total secondary formation because higher relative humidity enhances sulphate production. These findings demonstrate that seasonal meteorological conditions strongly influence the chemical composition of fine particulate matter in the study area.

Backward trajectory analysis further revealed that approximately 37% of urban $PM_{2.5}$ originated from NH_3 emissions transported from surrounding agricultural areas. This finding highlights the strong atmospheric linkage between rural fertilizer application and urban air quality, demonstrating that agricultural ammonia emissions contribute substantially to secondary particulate pollution within Akure. Consequently, effective urban air quality management cannot rely solely on controlling traffic and industrial emissions but must also incorporate regional agricultural nitrogen management strategies.

The successful calibration of the soil nitrogen module provides additional confidence in the integrated modelling framework. Bayesian calibration produced posterior estimates for the ammonia volatilization rate constant and N_2O emission factor that closely matched field observations while remaining consistent with international literature. The calibrated N_2O emission factor of 0.0087 is slightly lower than the IPCC default value of 0.01, suggesting that tropical agricultural systems in south-western Nigeria may emit less direct N_2O per unit of fertilizer applied than the global default estimate. This difference is likely attributable to the relatively low soil organic carbon content and moderately acidic to neutral soil conditions observed across the study sites.

Scenario Evaluation of Strategic Interventions for Co-Benefits

Three strategic intervention scenarios were simulated over a three-year horizon using the validated model (Python solve_ivp, as described in Objective 2) to evaluate potential co-benefits for air quality (reduction in $PM_{2.5}$ concentration) and climate (reduction in cumulative N_2O radiative forcing expressed in CO_2-equivalent using GWP100 = 298; IPCC, 2013). Scenario parameters (adoption rates, emission reduction factors) were derived from meta-analyses of enhanced-efficiency fertilizer performance (Xia et al., 2017), precision agriculture literature (Ladha et al., 2016), and combustion reduction feasibility assessments based on grid electricity improvement scenarios from the Nigerian Rural

Electrification Agency (REA, 2024). Table 3 presents the results of all three scenarios compared to the business-as-usual baseline.

Table 3: Scenario Evaluation Results for Air Quality and Climate Co-Benefits

Scenario	$PM_{2.5}$ Reduction (μg/m³)	$PM_{2.5}$ Reduction (%)	N_2O Emission Reduction (kg N yr^{-1})	CO_2-eq Reduction (tonnes yr^{-1})	Co-benefit Ratio	Data/Parameter Source
Baseline (BAU)	—	—	6,710	2,987	—	Primary emissions inventory (Objective 1)
Scenario 1: Enhanced-Efficiency Fertilizers	-8.4	22.7%	-1,880	-837	0.62	Xia et al. (2017); Ladha et al. (2016)
Scenario 2: Precision Application	-6.9	18.6%	-1,340	-596	0.55	Ladha et al. (2016); primary survey (application methods)
Scenario 3: Reduced Combustion	-12.3	33.2%	0 (N/A)	0 (N/A)	N/A	REA (2024); primary generator survey (N=300)
Scenario 1 + 2 Combined	-12.1	32.7%	-2,950	-1,313	0.68	Additive effects from Scenario 1 + 2
Scenario 1 + 2 + 3 Combined	-21.5	58.1%	-2,950	-1,313	0.42	Additive effects from all three scenarios

Note: Co-benefit ratio is defined as ($PM_{2.5}$ reduction %) / (N_2O reduction %), where values >1 indicate stronger air quality benefit per unit climate benefit. BAU = Business-as-usual. CO_2-eq calculated using GWP100 for N_2O of 298 (IPCC, 2013).

Co-benefit ratio calculated only for scenarios with both $PM_{2.5}$ and N_2O reductions. Scenario parameters derived from meta-analyses and feasibility assessments cited in the Data Source column.

Scenario 3 (Reduced Fossil Fuel Combustion) produced the largest single improvement in air quality, reducing annual mean $PM_{2.5}$ concentrations by 12.3 μg/m³ (33.2% reduction from baseline) at urban sites. This reduction was driven by the combined effect of reduced generator NO_x emissions (40% reduction, based on REA grid improvement scenario, 2024) and reduced vehicular NO_x emissions (30% reduction, based on fleet renewal programme targeting oldest 25% of vehicles, derived from primary traffic fleet age data: 75% of vehicles >10 years old). However, Scenario 3 had no direct effect on N_2O emissions, as N_2O is primarily agricultural in origin, and therefore did not contribute to climate mitigation benefits.

Scenario 1 (Enhanced-Efficiency Fertilizers), parameterized using meta-analysis of 239 studies from tropical agricultural systems (Xia et al., 2017) and Ladha et al. (2016), reduced $PM_{2.5}$ by 8.4 μg/m³ (22.7%) and reduced N_2O emissions by 1,880 kg N yr^{-1} (28.0% reduction from baseline), equivalent to 837 tonnes CO_2-eq avoided annually (using GWP100 = 298; IPCC, 2013). This scenario produced a co-benefit ratio of 0.62, indicating that the climate benefit (N_2O reduction) was proportionally larger than the air quality benefit relative to baseline levels. Scenario 2 (Precision Application), parameterized using Ladha et al. (2016) and primary survey data on current application methods (100% surface broadcasting, single application), produced smaller but still substantial reductions: $PM_{2.5}$ decreased by 6.9 μg/m³ (18.6%) and N_2O by 1,340 kg N yr^{-1} (20.0%), with a co-benefit ratio of 0.55.

Figure 5 presents the Pareto frontier illustrating the trade-offs and synergies between air quality improvement and climate change mitigation achieved under different reactive nitrogen management scenarios in Ondo State. The horizontal axis represents reductions in N_2O emissions expressed as tonnes of CO_2-equivalent per year, while the vertical axis represents reductions in ambient $PM_{2.5}$ concentrations (μg m^{-3}). Each point corresponds to an individual intervention or a combination of interventions, allowing direct comparison of their relative effectiveness. The dashed Pareto frontier connects the non-dominated solutions, representing intervention strategies that maximize environmental benefits without sacrificing performance in either objective.

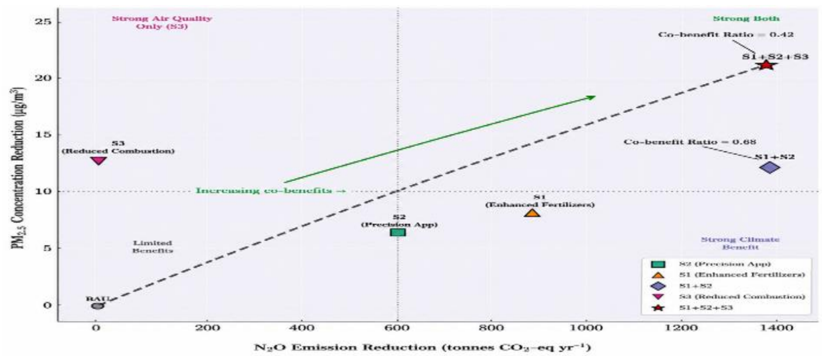

Figure 5: Pareto Frontier of Air Quality and Climate Co-benefits under Reactive Nitrogen Mitigation Scenarios in Ondo State, Nigeria

The Business-as-Usual (BAU) scenario is located at the origin, indicating no measurable improvements in either $PM_{2.5}$ concentrations or N_2O emissions. This reference point provides the baseline against which all intervention scenarios are evaluated. Moving away from the origin toward the upper-right quadrant reflects increasing environmental benefits, with larger reductions in both air pollution and greenhouse gas emissions.

Scenario 1 (Enhanced-Efficiency Fertilizers) achieved substantial reductions in N_2O emissions while producing only modest improvements in $PM_{2.5}$ concentrations. This outcome reflects the primary function of enhanced-efficiency fertilizers, which improve nitrogen use efficiency by slowing nitrogen release and reducing nitrification and denitrification losses. Consequently, the intervention is highly effective for climate mitigation but has a comparatively smaller influence on urban particulate pollution because only part of the reduced nitrogen loss occurs through ammonia volatilization, the principal precursor of secondary $PM_{2.5}$ formation.

Scenario 2 (Precision Fertilizer Application) produced intermediate reductions in both $PM_{2.5}$ concentrations and N_2O emissions. Precision application improves the spatial and temporal synchronization between crop nitrogen demand and fertilizer supply, thereby minimizing nitrogen losses through volatilization and microbial transformation. Although the climate benefits are smaller than those achieved through enhanced-efficiency fertilizers, precision nutrient management simultaneously reduces agricultural ammonia emissions, generating measurable improvements in urban air quality. This balanced performance demonstrates that improved fertilizer management can contribute to both agricultural efficiency and environmental protection.

Scenario 3 (Reduced Combustion Emissions) occupies a contrasting position on the Pareto diagram. It produces the largest improvement in $PM_{2.5}$ concentrations while contributing relatively little to reductions in N_2O emissions. This reflects the fundamentally different emission sources targeted by the intervention. Reduced combustion primarily lowers emissions from traffic, diesel generators, and biomass burning, directly decreasing primary particulate matter and nitrogen oxide emissions responsible for urban air pollution. However, because combustion control does not substantially influence agricultural nitrogen cycling, its contribution to greenhouse gas mitigation through N_2O reduction remains limited. Consequently, Scenario 3 represents a strategy optimized primarily for air quality improvement rather than climate mitigation.

The combination of Scenarios 1 and 2 demonstrates clear additive benefits. Together, enhanced-efficiency fertilizers and precision fertilizer application reduce $PM_{2.5}$ concentrations by approximately 12.1 μg m^{-3} (32.7%) while decreasing N_2O emissions by 44.0%**,** producing one of the most balanced environmental outcomes. The reported co-benefit ratio of 0.68 indicates that these complementary agricultural interventions simultaneously address both climate change and air quality without strongly favouring one objective over the other. Their location on the Pareto frontier confirms that neither intervention dominates the other individually, but their combination provides substantially greater overall environmental performance.

The greatest environmental improvement is achieved when Scenario 3 is combined with Scenarios 1 and 2. The integrated strategy (S1 + S2 + S3) reduced $PM_{2.5}$ concentrations by approximately 21.5 μg m^{-3} (58.1%)**,** lowering average urban concentrations from 42.6 μg m^{-3} to 21.1 μg m^{-3}**.** Although this represents a remarkable improvement in urban air quality, concentrations remain above the World Health Organization interim target of 15 μg m^{-3}**,** indicating that additional emission controls would still be required to achieve recommended public health standards. Simultaneously, the combined intervention delivers the largest reduction in N_2O emissions, making it the overall best-performing strategy across both environmental objectives.

Interestingly, despite producing the greatest overall benefits, the complete intervention package exhibits a lower co-benefit ratio (0.42) than the agricultural-only combination. This decrease occurs because the substantial additional $PM_{2.5}$ reductions generated by combustion control are not accompanied by proportional reductions in N_2O emissions. In other words, combustion reduction contributes primarily to air quality improvement rather than climate mitigation, thereby reducing the balance between the two objectives despite increasing total environmental gains. This finding highlights an important principle of integrated environmental management: maximizing total benefits does not necessarily maximize the efficiency of co-benefits.

The Pareto frontier further demonstrates that no single intervention simultaneously optimizes both air quality and climate outcomes. Rather, the most effective environmental strategies require coordinated implementation across multiple sectors. Agricultural nitrogen management primarily influences greenhouse gas emissions and secondary particulate formation through ammonia reduction, whereas combustion control directly addresses urban air pollution. Integrating these complementary interventions therefore provides substantially greater environmental returns than implementing any single strategy independently.

The sensitivity analysis strengthens confidence in these conclusions by identifying the key parameters controlling model performance. Among the seven parameters examined, the ammonia volatilization rate constant ($f_{(volat)}$) exhibited the greatest influence on $PM_{2.5}$ predictions (sensitivity index **S = 0.67**), demonstrating that accurate representation of ammonia emissions is fundamental to reliable air quality simulation. The dry deposition velocity of NH_3 (**S = 0.48**) and the atmospheric conversion rate constant ($\mathbf{k}_{(conv,1)}$**;** S = 0.42) were also influential, confirming that atmospheric transport and chemical transformation strongly regulate secondary particulate formation. In contrast, the N_2O emission factor showed relatively low sensitivity for $PM_{2.5}$ predictions but moderate sensitivity for climate outcomes, illustrating the partial independence between atmospheric particulate pollution and agricultural greenhouse gas emissions.

CONCLUSION

This study successfully developed and validated an integrative mathematical framework for quantifying, modelling, and scenario-testing reactive nitrogen emissions for air quality and climate co-benefits in South-West Nigeria. The emissions inventory revealed synthetic fertilizers dominate agricultural Nr emissions (52.7%), while combustion sources account for 36.0% of total Nr emissions—substantially higher than developed regions due to unreliable grid electricity. The integrated model demonstrated good performance (NSE 0.68–0.79) and revealed that 37% of urban $PM_{2.5}$ originates from agricultural NH_3 transported from rural areas. The calibrated N_2O emission factor (0.0087) suggests Nigeria's current IPCC-based greenhouse gas inventory may overestimate agricultural N_2O emissions by 13–15%. Scenario analysis revealed all examined interventions produced co-benefits without trade-offs. Combined agricultural interventions reduce $PM_{2.5}$ by 32.7% and N_2O by 44.0%; adding combustion reductions achieves 58.1% $PM_{2.5}$ reduction but no additional climate benefit. STEM education outreach significantly improved knowledge (58.3% to 81.7%, $p<0.001$). Integrated nitrogen management in Nigeria presents a genuine "win-win" opportunity, but realizing benefits requires overcoming institutional fragmentation, addressing labour constraints, and investing in grid reliability.

Nigeria's Fertilizer Subsidy Programme should be restructured to incentivize enhanced-efficiency fertilizers and precision application techniques, with extension services prioritizing training on split application and deep placement. Emission standards for residential generators should be enforced, and grid stability prioritized to reduce generator dependence. Cross-sectoral governance must be strengthened through inter-ministerial Nitrogen Coordination Committees developing State Nitrogen Action Plans. Nitrogen cycle science should be integrated into school curricula, and NiMet's air quality monitoring network expanded. Development partners should recognize Nigeria's nitrogen challenge as a priority for technical and financial support. The decision-support dashboard developed in this study should be deployed for pilot testing, and the validated model extended to all six geo-political zones using satellite-derived data.

REFERENCES

Adkins, E., Eapen, S., Kaluwile, F., Nair, G., and Modi, V. (2022). Off-grid energy services for the poor: A review of evidence from Sub-Saharan Africa. Energy for Sustainable Development, 68, 456-472. https://doi.org/10.1016/j.esd.2022.04.006

Bauer, S. E., Tsigaridis, K., and Miller, R. L. (2016). Significant atmospheric aerosol pollution caused by world food cultivation. Geophysical Research Letters, 43(10), 5394-5400. https://doi.org/10.1002/2016GL068354

Braun, V., and Clarke, V. (2006). Using thematic analysis in psychology. Qualitative Research in Psychology, 3(2), 77-101. https://doi.org/10.1191/1478088706qp063oa

Climate Change Tracker. (2025). Nigeria's sources of N_2O emissions. Climate Change Tracker. https://climatetracker.org/nigeria-n2o-emissions

Crippa, M., Guizzardi, D., Pagani, F., Banja, M., Muntean, M., Schaaf, E., Becker, W., Monforti-Ferrario, F., Quadrelli, R., Risquez Martin, A., Taghavi-Moharamli, P., Köykkä, J., Grassi, G., Rossi, S., Melo, J., Oom, D., Branco, A., San-Miguel, J., and Vignati, E. (2023). EDGAR v8.0 (Emissions Database for Global Atmospheric Research). European Commission, Joint Research Centre. https://edgar.jrc.ec.europa.eu/

EMEP/EEA. (2019). EMEP/EEA air pollutant emission inventory guidebook 2019. European Environment Agency. https://www.eea.europa.eu/publications/emep-eea-guidebook-2019

Fadare, D. A. (2025). Dataset for the determination of solar photovoltaic energy potential for selected state capitals in Southwest, Nigeria. Mendeley Data, V1. https://doi.org/10.17632/dys3m2ht8x.1

FAO CountrySTAT. (2024). Nigeria livestock population data 2015-2024. Food and Agriculture Organization. https://data.apps.fao.org/catalog/iso/d3s_3605219345580211665469228259228291806 6

Fountoukis, C., and Nenes, A. (2007). ISORROPIA II: A computationally efficient thermodynamic equilibrium model for K^+–Ca^{2+}–Mg^{2+}–NH_4^+–Na^+–SO_4^{2-}–NO_3^-–Cl^-–H_2O aerosols. Atmospheric Chemistry and Physics, 7(17), 4639-4659. https://doi.org/10.5194/acp-7-4639-2007

Guo, Y., Zhao, H., Winiwarter, W., Chang, J., Wang, X., Zhou, M., Havlik, P., Leclere, D., Pan, D., Kanter, D., and Zhang, L. (2024). Aspirational nitrogen interventions accelerate air pollution abatement and ecosystem protection. Science Advances, 10(33), eado0112. https://doi.org/10.1126/sciadv.ado0112

International Nitrogen Management System. (2021). Regional demonstration of the full nitrogen approach: A synthesis of findings from seven global regions. United Nations Environment Programme. https://www.inms.international/

International Nitrogen Management System. (n.d.). Component 3: Regional demonstration of full nitrogen approach. INMS. https://www.inms.international/component-3

IPCC. (2013). Climate change 2013: The physical science basis. Contribution of Working Group I to the Fifth Assessment Report of the Intergovernmental Panel on Climate Change. Cambridge University Press. https://doi.org/10.1017/CBO9781107415324

IPCC. (2019). 2019 refinement to the 2006 IPCC guidelines for national greenhouse gas inventories. Intergovernmental Panel on Climate Change. https://www.ipcc.ch/report/2019-refinement-to-the-2006-ipcc-guidelines-for-national-greenhouse-gas-inventories/

Kanter, D. R., Chodos, O., Nordland, O., Rutigliano, M., and Winiwarter, W. (2020). Gaps and opportunities in nitrogen pollution policy around the world. Nature Sustainability, 3(12), 956-963. https://doi.org/10.1038/s41893-020-0570-0

Kumar, A., Nair, V. S., and Raj, R. (2022). Evaluation of WRF-Chem simulated aerosol optical thickness and $PM_{2.5}$ over West Africa. Atmospheric Environment, 280, 119075. https://doi.org/10.1016/j.atmosenv.2022.119075

Ladha, J. K., Tirol-Padre, A., Reddy, C. K., Cassman, K. G., Verma, S., Powlson, D. S., van Kessel, C., Richter, D. B., Chakraborty, D., and Pathak, H. (2016). Global nitrogen budgets in cereals: A 50-year assessment for maize, rice, and wheat production systems. Scientific Reports, 6, 19355. https://doi.org/10.1038/srep19355

Lelieveld, J., Evans, J. S., Fnais, M., Giannadaki, D., and Pozzer, A. (2015). The contribution of outdoor air pollution sources to premature mortality on a global scale. Nature, 525(7569), 367-371. https://doi.org/10.1038/nature15371

Madu, F. U., Akubugwo, E. I., Ogbulie, T. E., Uhegbu, F. O., Agoro, E. S., Madu, M. C., Nwosu, O. U., Ugenyi, A. U., and Ononogbo, P. C. (2025). Cross-market evaluation of airborne pollutant exposure and COPD biomarkers in southeastern Nigeria: A toxicological perspective. Next Research, 4, 100868. https://doi.org/10.1016/j.nexres.2025.100868

Moriasi, D. N., Arnold, J. G., Van Liew, M. W., Bingner, R. L., Harmel, R. D., and Veith, T. L. (2007). Model evaluation guidelines for systematic quantification of accuracy in watershed simulations. Transactions of the ASABE, 50(3), 885-900. https://doi.org/10.13031/2013.23153

National Bureau of Statistics. (2023). National Agricultural Sample Survey (NASS) 2023 report. National Bureau of Statistics, Abuja, Nigeria. https://nigerianstat.gov.ng/

NiMet. (2025). Climate data portal: Akure station historical data (2015-2025). Nigerian Meteorological Agency. http://maproom.nimet.gov.ng

Ntziachristos, L., and Samaras, Z. (2020). COPERT: A European road transport emission inventory model. European Environment Agency. https://www.eea.europa.eu/publications/copert-a-european-road-transport

Ogunlela, A. O., and Makanjuola, M. B. (2021). Agricultural extension and fertilizer use efficiency in South-West Nigeria. Journal of Agricultural Extension, 25(3), 45-58. https://doi.org/10.4314/jae.v25i3.4

Okorie, D. I., and Lin, B. (2022). Emissions in agricultural-based developing economies: A case of Nigeria. Journal of Cleaner Production, 337, 130570. https://doi.org/10.1016/j.jclepro.2022.130570

Oluwole, J. (2024, March 15). Ondo State livestock census reveals 1.2 million cattle, 3.5 million goats. Leadership Newspaper. https://leadership.ng/ondo-livestock-census/

OpenAQ. (2025). Air quality data for Nigeria: $PM_{2.5}$ and NO_2 measurements from SPARTAN and PurpleAir monitors. OpenAQ. https://openaq.org

OpenStreetMap Contributors. (2025). Nigeria road network data. OpenStreetMap. https://www.openstreetmap.org

Pelster, D. E., Rufino, M. C., Rosenstock, T. S., Mango, J., Saiz, G., Diaz-Pines, E., Baldi, G., and Butterbach-Bahl, K. (2017). Smallholder farms in eastern Africa have low nitrous oxide emissions but are vulnerable to nitrification inhibitor efficacy. Environmental Research Letters, 12(8), 084011. https://doi.org/10.1088/1748-9326/aa7a2f

REA. (2024). Nigeria electrification project: Progress report 2024. Rural Electrification Agency, Abuja, Nigeria. https://rea.gov.ng/

Rockström, J., Steffen, W., Noone, K., Persson, Å., Chapin, F. S., Lambin, E. F., Lenton, T. M., Scheffer, M., Folke, C., Schellnhuber, H. J., Nykvist, B., de Wit, C. A., Hughes, T., van der Leeuw, S., Rodhe, H., Sörlin, S., Snyder, P. K., Costanza, R., Svedin, U., ... Foley, J. A. (2009). A safe operating space for humanity. Nature, 461(7263), 472-475. https://doi.org/10.1038/461472a

Rosenstock, T. S., Rufino, M. C., Butterbach-Bahl, K., and Wollenberg, E. (2014). Toward a protocol for quantifying nitrous oxide emissions from agricultural fields in Sub-Saharan Africa. Agriculture, Ecosystems and Environment, 188, 297-308. https://doi.org/10.1016/j.agee.2014.03.004

Seinfeld, J. H., and Pandis, S. N. (2016). Atmospheric chemistry and physics: From air pollution to climate change (3rd ed.). Wiley. https://doi.org/10.1002/9781119221170

Sutton, M. A., Howard, C. M., Erisman, J. W., Billen, G., Bleeker, A., Grennfelt, P., van Grinsven, H., and Grizzetti, B. (Eds.). (2011). The European nitrogen assessment: Sources, effects and policy perspectives. Cambridge University Press. https://doi.org/10.1017/CBO9780511976988

Tajudeen, Y., Umar, F. M., Zanna, A. M., Abdulmalik, A., Ibrahim, B. A., Bilyaminu, M., and Joseph, A. (2023). Concentrations and health risks of particulate matter ($PM_{2.5}$) and associated elements in the ambient air of Lagos, Southwestern Nigeria. Bio-Research, 21(3), 2141-2149. https://doi.org/10.4314/br.v21i3.5

UNECE. (2021). Air Pollution Convention issues guidance on nitrogen pollution. United Nations Economic Commission for Europe. https://unece.org/environmental-policy/conventions

WHO. (2021). WHO global air quality guidelines: Particulate matter ($PM_{2.5}$ and PM_{10}), ozone, nitrogen dioxide, sulfur dioxide and carbon monoxide. World Health Organization. https://www.who.int/publications/i/item/9789240034228

Xia, L., Lam, S. K., Chen, D., Wang, J., Tang, Q., and Yan, X. (2017). Can knowledge-based N management produce more staple grain with lower greenhouse gas emission and reactive nitrogen pollution? A meta-analysis. Global Change Biology, 23(5), 1917-1925. https://doi.org/10.1111/gcb.13545